Dipole-directed assembly of lines of 1,5-dichloropentane on silicon substrates by displacement of surface charge

K. R. HARIKUMAR[1], TINGBIN LIM[1], IAIN R McNAB[1], JOHN C. POLANYI[1]*, LINDA ZOTTI[2], SERGE AYISSI[2] AND WERNER A. HOFER[2]

[1]Department of Chemistry and Institute of Optical Sciences, University of Toronto, 80 St George Street, Toronto, Ontario M5S 3H6, Canada
[2]Surface Science Research Centre, University of Liverpool, Liverpool L69 3BX, UK
*e-mail: jpolanyi@chem.utoronto.ca

One-dimensional nanostructures at silicon surfaces have potential applications in nanoscale devices. Here we propose a mechanism of dipole-directed assembly for the growth of lines of physisorbed dipolar molecules. The adsorbate chosen was a halide, in preparation for the patterned imprinting of halogen atoms. Using scanning tunnelling microscopy, physisorbed 1,5-dichloropentane on Si(100)-2×1 was shown to self-assemble at room temperature into molecular lines that grew predominantly perpendicular to the Si-dimer rows. Line formation was triggered by the displacement of surface charge by the dipolar adsorbate. Experimental and simulated scanning tunnelling microscopy images were in agreement for a range of positive and negative bias voltages. The geometry of the physisorbed molecules and nature of their binding were evident from the scanning tunnelling microscopy images, as interpreted by scanning tunnelling microscopy simulation.

Over the last decade many systems have been identified that yield self-assembled atomic or molecular lines on semiconductors. All these nanolines were formed as a result of covalent bonding within or at the surface. Here we describe a method for the formation of self-assembled molecular lines at room temperature on a bare Si(100)-2×1 surface using the novel approach of dipole-directed assembly (DDA), shown here for 1,5-dichloropentane (DCP). The adsorbate DCP was chosen because the Cl⋯Cl separation in a favoured configuration is ~4 Å, closely matching the 3.8 Å Si⋯Si separation between adjacent Si-dimer pairs, hence offering the possibility of physisorption in a bridging configuration, with the Cl atoms located over adjacent Si atoms. The method has also been applied in initial studies on 1-chloropentane, 1-fluoropentane and 1-chlorododecane.

Earlier works report the study of bismuth nanolines[1–6] and rare-earth silicide nanowires[7–16] on Si(100)-2×1 using scanning tunnelling microscopy (STM). These lines, of up to 500 nm in length, grew perpendicular to the Si-dimer rows. The lines were formed at high substrate temperatures, ~600 °C, by sub-surface reconstruction induced by covalent bonding. Shorter nanolines formed on Si(100) from group II, III and IV metals (for example, Mg, Al and Sn) have also been reported[17–23]. Lines of physisorbed molecules have been self-assembled through intermolecular hydrogen-bonding on smooth graphite (see, for example, ref. 24) and metal surfaces (see, for example, ref. 25) but not on Si(100).

Chemical chain reactions have also been used to grow nanolines[26–30]. Growth occurred along[26–28] and across[29,30] the dimer rows of H-terminated Si(100), initiated from a dangling-bond site[26–30]. Recently, self-assembled molecular lines were formed on a bare Si(100)-2×1 surface perpendicular to the dimer rows[31], using a surface chain reaction initiated by pyrazine.

The adsorbate of the present work, DCP, has been shown by *ab initio* calculation to result in a dipole at the surface and to induce buckling of the Si-dimer pair of an adjacent row. This buckling favours the adsorption of a molecule at the buckled site. The second adsorbate molecule induces a further buckling in the next Si-dimer row and hence a new site favouring molecular adsorption, and so on, thereby propagating a line of intact physisorbed molecules, as observed. The direction of line growth is invariably opposite to the direction of the dipole. The predominant unidirectionality of the line growth is not explained *ab initio*; it is likely to have its origin in the tendency for the relief of surface strain to take place linearly along an axis of symmetry[32–35].

According to both theory and our STM experiments, the DCP molecules physisorbed at room temperature with their terminal Cl atoms interacting with adjacent Si-dimer atoms to one side of the same dimer row (that is, asymmetrically). The DCP molecular lines self-assembled unidirectionally in the direction of their asymmetric point of attachment, and thus opposed to the direction of the C−Cl dipoles. The direction of line growth was predominantly perpendicular to the dimer rows.

Simulations matched the STM images for both empty- and filled-state (positive and negative surface bias) images. Comparison of the STM images with the simulations yielded the adsorption geometry of the molecules and therefore the origin of the likely physisorptive interactions, C−Cl⋯Si, binding the DCP to Si atoms at the underlying surface.

A recent theoretical study[36,37] of the interactions of dipolar molecules with Si(100)-2×1 at high coverages of 0.5 and
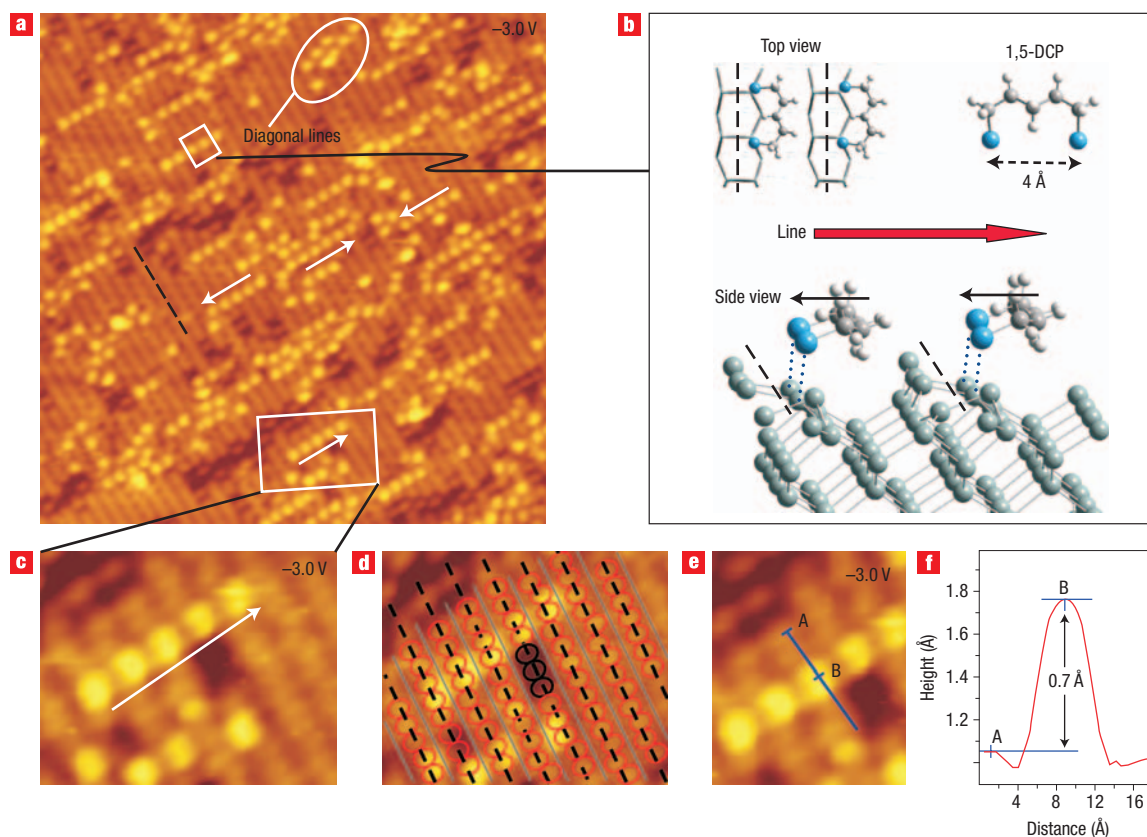
Figure 1 Self-assembled molecular nanolines at room temperature. a, A room-temperature STM image (270 × 270 Å) of a Si(100)-2×1 surface exposed to 1 L nominally (an uncorrected pressure of 5×10^{-9} torr, 200 s) of DCP. Lines of DCP are imaged as bright features mostly perpendicular to the Si-dimer rows, but with ~5% at 26° to the dimer rows (example circled). The direction of line growth is known, and is shown for several cases by white arrows. Individual DCP features (bright protrusions) lie to one side of the dimer rows. **b,** Perspective and top views (left inset). Black dashed lines denote the centre of the Si-dimer rows throughout, blue spheres denote Cl atoms and blue dotted lines the physisorption interaction. The black arrows indicate the adsorbate dipoles and the long red arrow points in the direction of line growth. A model of 1,5-DCP is shown in the right inset. **c,** Close-up (60 × 40 Å) of the nanoline taken from the white rectangle in **a. d,** Same view as in panel **c.** Red and black ellipses denote dimers and defects, respectively, black-dashed and grey lines indicate the centre of the ridges and the valleys of the dimer rows. From this picture it is evident that the molecular features (bright protrusions) lie to one side of the dimer rows (to the right as we have oriented panels **c−e**). A height profile taken along the blue line in the STM image **e** is shown in **f.** The point 'A' in the linescan denotes a Si dimer, and the highest point in profile 'B' corresponds to the midpoint of the molecular feature in this line. At this bias (−3 V), the average height of the molecular feature with respect to the Si dimer is 0.7 Å. The dark features in the STM images are due mainly to missing-dimer defects.

1.0 monolayers predicted four types of important surface effects resulting in a preference for molecular absorbtion on neighbouring Si dimers of the row. However, these workers discounted the possibility of interaction between adjacent dimer rows, which is central to the present work.

RESULTS AND DISCUSSION

Figure 1a shows an STM image of Si(100)-2×1 exposed to 1 L (uncorrected; see Methods for definition of units Langmuir) of 1,5-DCP at room temperature. Intact molecules physisorbed onto the Si surface and self-assembled to form lines predominantly perpendicular to the dimer rows. Approximately 5% of the lines grew diagonally.

The molecule–molecule separation distance was 7.7 Å, in agreement with the long axis of the Si(100)-2×1 unit cell. The nanolines consisted of 4−6 molecules on average, 40−50 Å long and 4 Å wide. Lines were, however, observed with up to 12 molecules (90−100 Å long). Increased line length required low dose rates (see later). The STM images suggest that the

individual DCP molecules changed their C−Cl bond direction under the influence of the surface to align their Cl atoms with two Si-dimer atoms, one from each adjacent dimer pair to one side of a dimer row, as shown in Fig. 1b. The width of the DCP lines is comparable with the dimer–dimer distance along a row, that is, 3.8 Å. This structure was confirmed by the *ab initio* calculations presented below.

The bright features characteristic of the physisorbed molecules did not bridge the dimer rows (Fig. 1c,d). This is in contrast to the molecular lines formed by pyrazine on bare Si(100)-2×1 midway between two dimer rows, because the pyrazine adsorbate was bound covalently to the adjacent rows[31]. The DCP lines have an experimental height of 0.7 Å for −3 V (Fig. 1f). This agrees with the simulation, which suggests protrusions of ~0.8 Å in the density contour for this voltage.

The DCP molecules involved in DDA physisorbed and self-assembled intact. The evidence for physisorption of intact DCP was that the molecular lines desorbed at elevated temperature (> ~ 200 °C), leaving no residue at the surface. In contrast, a covalently bound Si−Cl bond formed by reaction at the surface

will desorb only above 500 °C (refs 38, 39, 40). Further, DCP molecular lines were thermally stable up to ~200 °C. Above 200 °C, over time, a fraction underwent reaction, severing a C−Cl bond to give Cl−Si at the surface, characterized by circular bright spots in the STM image. The bright spots were the Si dangling bonds adjacent to a reacted Cl (Cl−Si). The remainder of the DCP adsorbate desorbed from the surface at 200 °C without chemical reaction, leaving no residue, as expected for a physisorbed molecule.

As noted, higher dose rates gave shorter lines, and lower dose rates longer lines; dosing at 1×10^{-9} torr produced lines of 8−10 molecules, whereas 1×10^{-8} torr gave lines of 3−5 molecules. The STM images indicated that the lines invariably originated in dimeric DCP, $(DCP)_2$, a characteristic large bright feature evident at the head of the line in Fig. 2. At the highest dose rate only this bright feature was observed.

Previously, we found that chloroalkanes on Si(111)-7×7 predominantly formed dimers at high dose rates, physisorbing horizontally on Si(111)-7×7 and Si(100)-2×1 in contact with the surface[41]. This geometry gave additional binding from the contact of CH_2 with the underlying Si surface, rendering the horizontal molecules more stable in their adsorbed state[42–44]. On heating, the dimeric $(DCP)_2$ was found, as expected from its multiple points of attachment, to be more strongly bound to the surface than the monomer.

In the present experiment, line length was limited by a kinetic competition between dimer formation (the start of a new line) and attachment of a monomer to an existing line (resulting in line growth). Because of the quadratic dependence on monomer concentration for dimer formation[45], high dose rates favoured the formation of many dimers, and hence shorter lines.

At room temperature, we observed no features that could be ascribed to single monomeric DCP molecules in the adsorbed state, due, presumably, to their high mobility. The observed molecular lines originated in a stable $(DCP)_2$ dimer—the 'anchor' for that line. The lines propagated through linear self-assembly of a succession of DCP monomers, which, although unstable individually, were highly stable when self-assembled, even at elevated temperatures up to ~200 °C. At high resolution the lines in the room-temperature images gave evidence of terminating in a raised surface feature (Fig. 2), in agreement with expectations from the DDA model, presented in the following sections.

In other experiments DCP was dosed at a 100 °C Si(100)-2×1 surface using the same dose rate as in the room-temperature experiments. No nanolines were observed. Instead, reaction took place to yield exclusively halogen atoms. Once again, the remainder of the DCP molecule desorbed. Dosing at 100 °C gave a smaller coverage, in this case of Cl−Si, by a factor of between 10 and 12, than an equivalent dose at room temperature, indicating that the sticking probability was lower by this amount as compared with that at room temperature.

In Fig. 2a we show a high-resolution image of a single DCP line. The anchor, the DCP dimer $(DCP)_2$, is clearly visible, as are the individual DCP molecules in the line, and also the Si surface dimers and back bonds. The end of the line shows a severe perturbation of the Si dimers. Theory suggests that this perturbation is due to buckling of the surface originating in the dipole of the adsorbate (hence 'dipole-directed assembly') encouraging the adsorbtion of a further DCP molecule and so continuing line growth. Line growth is limited here by DCP coverage.

Figure 2c to f shows STM images of another DCP line, obtained with different negative and positive sample biases (left and right, respectively). The appearance of the line can be seen to be highly voltage-dependent. The corresponding left and right images were
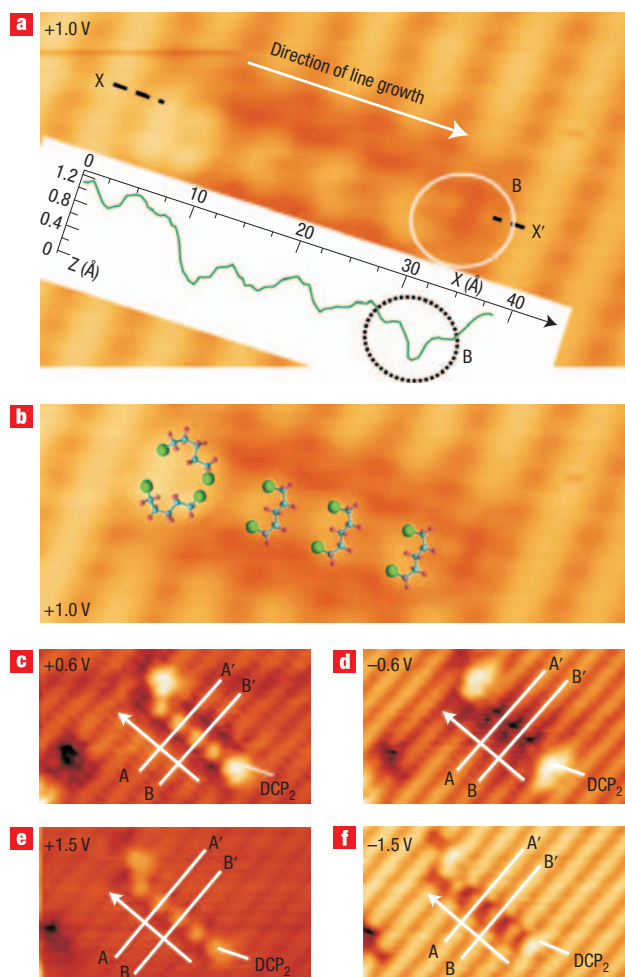

Figure 2 STM images of single nanolines. a, High-resolution image (50 × 30 Å) of a single DCP line with a line height profile (inset) taken along the line X−X′; the circled feature 'B' is the perturbation at the end of the line due to surface buckling. **b**, The image of panel **a** reproduced with ball and stick molecules superimposed, to scale, of $(DCP)_2$ and DCP over the corresponding features of the image. **c−f**, STM images (85 × 60 Å) of a further single DCP line at positive and negative voltages; panels **c** and **d** were recorded simultaneously as were panels **e** and **f**. An additional DCP dimer (unlabelled) is visible at the left, adjacent to the line. The white lines A−A′ and B−B′ marked in each image represent the same features, the ridges of adjacent dimer rows in **c−f**. In positive bias the DCP line always appears bright relative to the dimer rows. The positive-bias images (**c** and **e**) show the well-known contrast reversal at and above +1.5 V bias; A−A′ and B−B′ then appear as valleys rather than ridges. In negative-bias images the DCP line appears dark relative to the dimer rows, brightening as the bias goes to larger negative values. The direction of line growth is indicated by white arrows; line growth can be seen to begin with a DCP dimer $(DCP)_2$. Dark trenches are observed to both sides of the DCP lines of bright molecules; this is due to pinning of adjacent dimers (see text and Fig. 4). At high bias (positive and negative), the DCP dimers can be seen to be almost indistinguishable from individual DCP molecules.

taken simultaneously with opposite biases in alternate line scans. In the filled state (negative surface bias, Fig. 2d and f), as the magnitude of bias was increased the lines brightened. At sufficiently high negative bias, starting at −2 V (not shown), the molecular lines were brighter than the Si-dimer rows; at lower negative biases they appeared darker than the Si-dimer rows. The
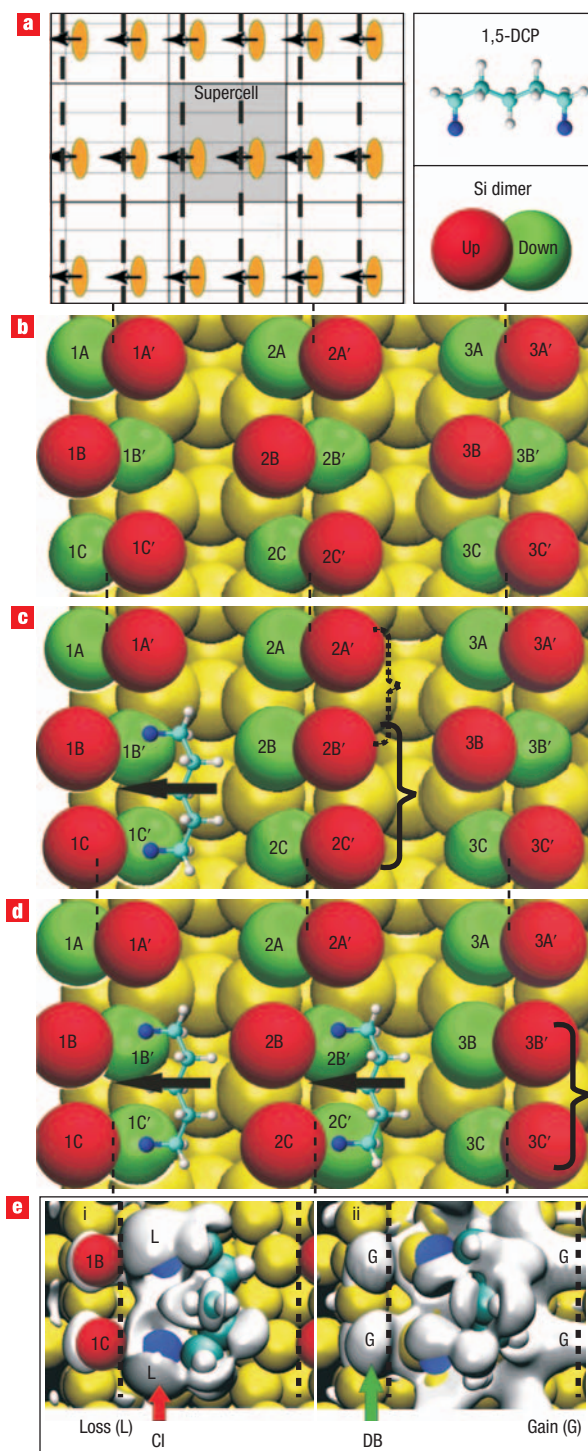
Si atoms 1B′ and 1C′ are down, and 1B and 1C are up. In row 2, 2B′ and 2C′ are up, 2B and 2C are down. The brackets indicate favoured pairs of adsorption sites for the second DCP molecule. **d**, Attachment of the second molecule in row 2 repeats for rows 2 and 3 the process of surface-buckling shown for rows 1 and 2 in **c**. The third adsorbate molecule (not shown) will attach to the bracketed Si atoms collinear with the first two dipolar adsorbate molecules. **e**, Charge redistribution on adsorption of a DCP molecule. (i) Loss (L) in electronic density within the white contour shown ($-0.004e\,\mathrm{\AA}^{-3}$) and (ii) gain (G) in electronic density within the white contour ($+0.004e\,\mathrm{\AA}^{-3}$). Colour coding is as in the other panels. Cl indicates the approximate location of the halogen atom losing negative charge, and DB the location of the Si dangling bond (1B and 1C) gaining charge. The black dashed line denotes the centres of the Si dimer rows.

bright features comprising the lines of DCP in the STM images are calculated to be primarily due to the contribution from the alkyl chains made visible by the attached halogen atoms[46,47]. Figure 2c,e shows the well-known contrast reversal, in which the ridge of a dimer row appears bright below 1.5 V and dark above 1.5 V surface bias[48–50].

DENSITY FUNCTIONAL THEORY CALCULATIONS

To understand the formation of molecular lines on the surface we performed extensive density functional theory (DFT) simulations (see Methods). In Fig. 3 we show the details of the computed mechanism for line propagation. Figure 3b shows the state of the Si dimers p(2×2) on Si(100), which is in an unperturbed up–down Si-dimer pair configuration. The up and down Si atoms in the Si dimers are colour-coded red (up) and dark green (down). Generally, this configuration corresponds to an excess (up) and a depletion (down) of electron charge (see, for example, ref. 51). The two Si-dimer pairs of interest, on which the Cl atoms of the first DCP will physisorb, are labelled 1B′ and 1C′. The adsorption energy using a linear molecule in vacuum as the reference is 2.6 eV per molecule. The energy required to change the C−Cl bond direction from that in the gas-phase molecule to the configuration on the surface is approximately 0.2 eV. Calculation of a DCP dimer clearly showed buckling of the adjacent Si-dimer pair, as for the DCP monomer. Details of (DCP)$_2$ interaction with the surface will be published as part of a study of dimeric adsorbates and their DDA. The present discussion focuses on the (novel) mechanism of DCP monomer line propagation.

The attachment of a single DCP molecule at 1B′ and 1C′ on row 1 leads to a dipole, both because of a charge transfer from the Cl atoms of the DCP to adjacent Si dimers and the induced dipole of the molecule in its adsorbed configuration. This net dipole is directed perpendicular to the Si-dimer rows with a dipole strength of 4.85 D (debye) indicated by black arrows in Fig. 3 (we use the convention that the arrows point from positive to negative in the dipole). Figure 3c shows buckling of the Si dimers resulting from the adsorption of this first molecule. The computed charge redistribution consequent on DCP physisorption is shown in Fig. 3e; electron density has moved from the Cl atoms (adsorbed at Si atoms 1B′ and 1C′) to the other Si atoms of the same dimer pairs, 1B and 1C, which, consequently, are raised to the 'up' configuration (see previous paragraph). Owing to the electrostatic interaction between the dipole and the Si atoms of the adjacent row, no. 2 in Fig. 3, dimers 2A, 2A′; 2B, 2B′ and 2C, 2C′ flip as shown in Fig. 3c. This may be assisted by the inter-row charge transfer evident as 'tails' in the negative charge gain (G) at the right of Fig. 3e (ii). The Si-dimer reorientation leads to an energy gain of 140 meV and provides a preferential adsorption site for the next molecule in its mobile precursor state.

Figure 3 Mechanism of formation of the molecular line (theory). a, Schematic representation of the dipoles (short black arrows) responsible for buckling of the dimers. The locations of the molecules are represented by golden ellipses. The grey box represents the supercell slab used for the calculation. The black dashed lines denote the centres of the Si-dimer rows. The 1,5-DCP molecule and the colour-coded 'up' and 'down' Si dimer atoms are shown. **b**, Ground-state Si(100)-p2×2 surface. The dimer pairs are numbered 1A–1A′, 1B–1B′ and 1C–1C′ in the left dimer row, 2A–2A′, 2B–2B′ and 2C–2C′ in the adjacent dimer row and 3A–3A′, 3B–3B′ and 3C–3C′ in the third dimer row. The 'up' and 'down' dimers are colour-coded red and green. **c**, The computed buckling due to adsorption of a single molecule on row 1. The bonded
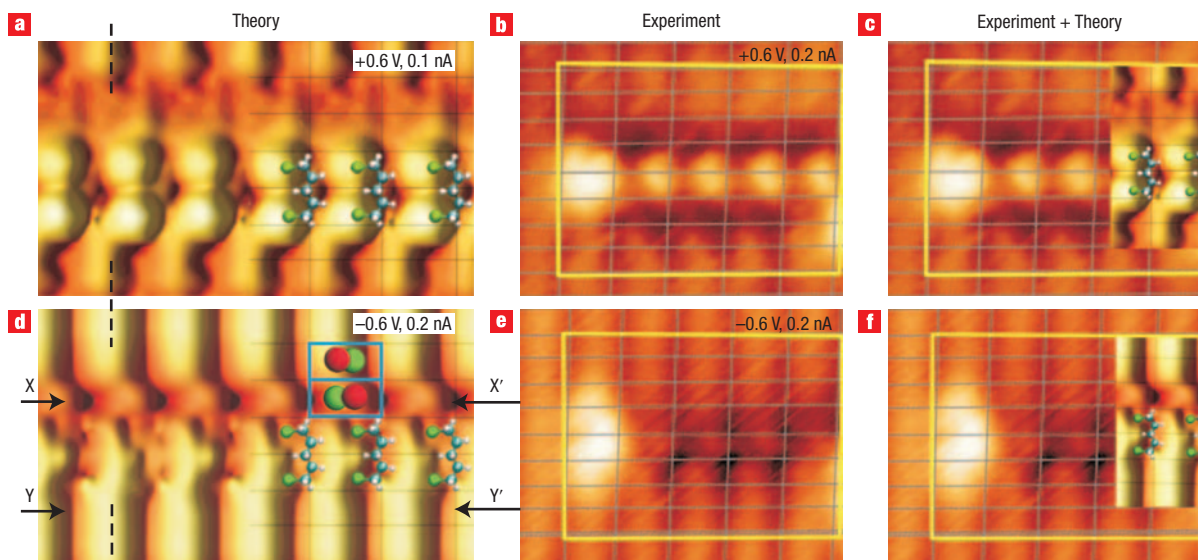
Figure 4 Comparison between theoretical and experimental images. a,d, Simulated STM images of DCP molecules arranged in lines on Si(100)-p(2×2) at +0.6 V (**a**) and −0.6 V (**d**) bias. Each rectangle in the grid represents a 2 × 1 unit cell (two of which are highlighted by blue rectangles in **d**, with up and down Si atoms coloured red and green); DCP molecules are drawn to scale at the right in the simulated images. The centres of the dimer rows in the simulated images are indicated by dashed lines (corresponding to the ridges of the dimer rows in the experimental images). In the simulated image of the empty state (**a**), bright protrusions are visible at the location of the Cl atoms. **b,e,** Images recorded at the same bias as the simulations (**a,d**); the appearance of the lines in the simulated images matches well with the appearance of the lines in the experimental STM images at the same bias. For the positive-bias image, theoretical simulations were made at half the experimental current (0.1 nA rather than 0.2 nA) so the features due to DCP appear enlarged relative to the experimental image. **c,f,** The simulated lines are shown superimposed on the experimental images. The dark arrows X−X′ and Y−Y′ in **d** show a line of darkness above the molecular line and a line of brightness below the molecular line (see text). The filled-state STM image at −0.6 V is shown in **e**; the lines appear darker at this bias, which matches the simulated image **d**.

The second DCP molecule can only attach at the elevated Si atoms (2B′, 2C′) due to steric hindrance from the first DCP. Subsequently the pair of Si atoms 2B′, 2C′ move down (Fig. 3d, green). This is accompanied by further reorientation at the adjacent Si-dimer row 3, with elevation of Si atoms 3B′ and 3C′, preparing a raised site for attachment of a third DCP (Fig. 3d, bracketed red atoms). The sequence then continues until the system either runs out of adsorbate or encounters a defect.

A second DCP molecule migrating across the surface could, alternatively (Fig. 3c) attach at the pair of Si atoms labelled 2A′ (raised) and 2B′ (raised). A growth direction perpendicular to the dimer rows is energetically favoured due to dipole interactions by about 80 meV per molecule relative to diagonal line growth. The difference in the adsorption energy is sufficient to make diagonal growth only ∼5% as likely as perpendicular growth, at room temperature, as is observed.

In the presence of two adsorbate molecules (Fig. 3d), line growth in general proceeds collinearly with these molecules; that is, the lines rarely wander from their initial propagation direction. A likely explanation is a tendency for strain to relieve itself linearly in the surface[34–37]. However, the growth of the line beyond two DCP molecules is beyond the limit of our supercell, and hence not calculable.

In summary, adsorbed molecules induce substantial dipoles (shown as black arrows pointing to the left in Fig. 3), which result from charge transfer to the surface and the dipole of the distorted DCP. Electrostatic interactions with this net dipole pin the Si dimers on the adjacent Si-dimer row, to the right in the figure, into their new configuration as detailed above, and propagate the line through self-assembly of additional DCP monomer molecules away from the direction of the initial induced dipole. This is the mechanism for DDA.

STM SIMULATIONS

In Fig. 4 we compare the simulated STM image with the experimental constant-current (0.2 nA) STM images at a sample bias of ±0.6 V. The calculated images reproduce the observation of a tip−surface distance of 6−7 Å. Images were simulated using a metal tip with a mono-atomic apex at a current of 0.2 nA (negative bias) and 0.1 nA (positive bias). The current contour in the positive regime is closer to the surface, so we had to decrease the contour value to obtain a closed contour surface (see Methods). Because the 4 × 4 supercell is too small to describe the boundary between the molecular lines and the dimer rows, we used a 4 × 6 supercell in all simulations. To analyse the effect of dimer buckling adjacent to the molecular rows we varied the supercell boundary. The Si dimers have the correct up−down orientation on one side (above, in the simulations of Fig. 4), but are flipped in the opposite direction on the other side (below, in the simulations of Fig. 4). At higher negative bias voltages (images not shown) we find that the protrusion due to the adsorbed molecules had its maximum at the position of the Cl atoms.

The computed images in Fig. 4d have darkness above the molecular line (X−X′) and brightness below (Y−Y′). The calculated darkness is due to the Si dimer being buckled in the opposite sense to the rest of its row, as shown in the blue-bounded insert. Brightness indicates that the Si dimer is buckled in the same sense as the rest of its row. Experimentally, in both positive and negative STM images at low bias (±0.6 V; Fig. 4b,e), we observed darkness at both sides of the line. It would appear that the dimers on both sides of the molecular rows are pinned, and the rest of the rows appear bright due to averaging of dimer positions at room temperature.

CONCLUSIONS

We report a novel DDA mechanism for the formation of physisorbed molecular lines at room temperature on a Si(100)-2×1 surface, as observed by STM and modelled by DFT calculation. Self-assembly resulted in lines of intact 1,5-DCP monomers of up to 12 molecules aligned predominantly perpendicular to the dimer rows, with a 5% minority at a 26° angle to the rows. Once a pair of molecules established a line direction, that direction was generally observed to be maintained invariable for all subsequent molecules in the line.

The mechanism of line propagation of DCP monomers was shown by DFT calculation to originate in the dipole of an adsorbed molecule, molecule 1, attached by its two halogen atoms to adjacent Si atoms along a dimer row. The dipole-induced charge transfer in the surface is perpendicular to the Si-dimer row. This transfer of charge resulted in buckling of adjacent dimer pairs in row 2, giving rise to an attractive site for molecule 2. A second DCP monomer was adsorbed adjacent to the first, further shifting the surface charge, thereby buckling row 3 and capturing a third DCP molecule along the extension of the line formed by the first two, so propagating the line.

At room temperature, DCP monomers are mobile on Si(100)-2×1. Line growth originated in a single dimer of $(DCP)_2$ (the anchor) through subsequent collinear assembly of the mobile DCP monomers. In the STM images the constituent DCP molecules of the line were displaced to the same side of successive Si-dimer rows as the direction of line growth, in agreement with theory. This direction of line growth by DDA is opposite to the direction of the individual DCP dipoles. Where line growth was limited by coverage, surface-buckling could be seen by STM in the Si-dimer row beyond the final DCP molecule of the line. Line termination was also observed to occur due to defective assembly, occasioned by a second dimer or by a surface defect.

A requirement for DDA is that the initial adsorbate molecule has a preferred adsorbate alignment on the surface and a dipole moment when adsorbed. The orientation of the adsorbate dipole, through the mediation of surface charge transfer, is opposite to the propagation direction of the self-assembled line. Further requirements are that the substrate be electrically polarizable, and that subsequent molecules to the first be sufficiently mobile to self-assemble. Charge transfer in the surface manifests itself, in the present case, as a buckling of the Si atoms of an adjacent dimer row of Si(100)-2×1.

The physisorbed dipolar molecular lines observed in this work were stable up to temperatures of ∼200 °C, without desorption or chemical reaction. The finding that mobile dipolar adsorbates can self-assemble into such robust lines under the influence of charge transfer to or from the substrate should be of interest in contexts ranging from nanoscale electronics to molecular biology.

METHODS

EXPERIMENTAL METHODS

Experiments were carried out at room temperature in ultrahigh vacuum (UHV) using two STM instruments (RHK400 and Omicron-VT) using phosphorous-doped (n-type, 0.01−0.02 Ω·cm, 250 ± 25 μm thick) Si(100) reconstructed to give Si(100)-2×1. The adsorbate 1,5-DCP (99.9 % pure, Aldrich) was subjected to repeated freeze−pump−thaw cycles before being introduced to the UHV chamber through a leak valve for background dosing. Exposures are reported in Langmuir (1 L = 1 × 10⁻⁶ torr s) measured with an uncorrected ion-gauge calibrated for N_2. The corrected doses would be ∼10 times lower than the stated doses[52]. The STM tips were made by a d.c. electrochemical etch of polycrystalline tungsten wire in a 2 M NaOH solution.

The scanning tunnelling microscopes were operated in the constant-current mode. All measurements were made with a tunnelling current of 0.2 nA. Samples

were cleaned in UHV by several cycles of d.c. heating to 1,240 °C for ∼1 min. The STM images of the surface cleaned in this way showed a (2 × 1) reconstruction and < 0.2% surface defects.

ELECTRONIC STRUCTURE SIMULATIONS

The ground-state electronic structure of one or two molecules on Si(100) was simulated with the Vienna Ab initio Simulation Package (VASP)[53,54] using ultrasoft pseudopotentials and the PW91 parameterization[55] of the exchange-correlation potential. The Si(100) slab contained eight layers, the bottom layer of which was passivated with hydrogen. We simulated 4 × 4 and 4 × 6 supercells, retaining the p(2×2) arrangement of the buckled dimers. The high number of layers was necessary to represent the high elasticity of the silicon lattice. Owing to the large number of atoms, we limited the simulations of the relaxed geometry to one k-point at the centre of the surface brillouin zone. The molecular adsorption site was determined by placing the bent molecules about 3 Å above the surface plane, with the molecular backbone parallel to the surface. The molecule, as well as three surface layers, were then fully relaxed until the forces on individual ions were less than 0.02 eVÅ⁻¹.

The molecular adsorption sites for one- and two-monomer DCP molecules in a 4 × 4 and 4 × 6 Si(100) supercell were calculated using several supercells: a single DCP molecule in a 4 × 4 supercell, two molecules in alignment perpendicular to the dimer rows, two molecules in diagonal alignment, and the same three arrangements of molecules in a 4 × 6 supercell. The alignment of adsorbate molecular dipoles is shown schematically in Fig. 3a. The grey box represents the supercell slab used for the calculation (not the surface unit cell).

CALCULATION OF DIPOLES

DFT calculation gives a zero dipole for the symmetric linear DCP molecule in the gas. The dipoles were calculated for a single molecule on the Si(100)-4×4 supercell using the dipole corrections implemented in our electronic structure code. For this simulation we first calculated the electron density of the molecules in the vacuum, then the density of the clean Si surface and finally the density of the complete system. Subtracting the density of the components from the density of the complete system yielded the charge transfer due to adsorption. The position of the dipole was subsequently placed at the median position between positive and negative charge accumulation, and the dipole moment was calculated using dipole corrections in (only) two dimensions along the surface plane. We found a dipole moment of 4.85 D per molecule perpendicular to the dimer rows.

SIMULATION OF STM IMAGES

The STM images for a current of 200 pA (negative bias) or 100 pA (positive bias) and a range of bias voltages were simulated using the electronic structure of the converged system, and the multiple scattering approach implemented in bSKAN[56,57]. To improve the accuracy we used a k-point set of 3 × 3 special k-points in the final electronic structure simulations, as also for the STM simulations. To obtain a closed contour surface in the simulation, the current value in the positive bias regime had to be reduced.

References

1. Naitoh, M., Shimaya, H., Nishigaki, S., Oishi, N. & Shoji, F. Scanning tunneling microscopy observation of bismuth growth on Si(100) surfaces. *Surf. Sci.* **377−379,** 899−903 (1997).
2. Naitoh, M., Shimaya, H., Nishigaki, S., Oishi, N. & Shoji, F. Scanning tunneling microscopy observation of Bi-induced surface structures on the Si(100) surface. *Surf. Sci.* **482−485,** 1440−1444 (2001).
3. Owen, J. H. G., Miki, K. & Bowler, D. R. Self-assembled nanowires on semiconductor surfaces. *J. Mater. Sci.* **41,** 4568−4603 (2006).
4. MacLeod, J. M. & McLean, A. B. Single 2 × 1 domain orientation on Si(100) surfaces using a periodic Bi line arrays. *Phys. Rev B* **70,** 041306 (2004).
5. MacLeod, J. M., Miwa, R. H., Srivastava, G. P. & McLean, A. B. The electronic origin of contrast reversal in bias-dependent STM images of nanolines. *Surf. Sci.* **576,** 116−122 (2005).
6. Preinesberger, C., Vandre, S., Kalka, T. & Dahne-Preitsch, M. Formation of dysprosium silicide wires on Si(001) . *J. Phys. D* **31,** L43−L45 (1998).
7. Chen, Y., Ohlberg, D. A. A. & Williams, R. S. Nanowires of four epitaxial hexagonal silicides grown on Si(001). *J. Appl. Phys.* **91,** 3213−3218 (2002).
8. Nogami, J., Liu, B. Z., Katkov, M. V., Ohbuchi, C. & Birge, N. O. Self-assembled rare earth silicide nanowires on Si(001). *Phys. Rev. B* **63,** 233305 (2001).
9. Liu, B. Z. & Nogami, J. Growth of parallel rare earth silicide nanowire arrays on vicinal Si(001). *Nanotechnology* **14,** 873−877 (2003).
10. Liu, B. Z. & Nogami, J. An STM study of the Si(001)(2×4)-Dy surface. *Surf. Sci.* **488,** 399−405 (2001).
11. Ohbuchi, C. & Nogami, J. Holmium growth on Si(001): Surface reconstructions and nanowire formation. *Phys. Rev. B* **66,** 165323 (2002).
12. Katkov, M. V. & Nogami, J. Yb and Nd growth on Si(001). *Surf. Sci.* **524,** 129−136 (2003).

13. Ohbuchi, C. & Nogami, J. Samarium induced surface reconstructions of Si(001). *Surf. Sci.* **579**, 157–165 (2005).

14. Harrison, B. C. & Boland, J. J. Real-time STM study of inter-nanowire reactions: GdSi$_2$ nanowires on Si(100). *Surf. Sci.* **594**, 93–98 (2005).

15. Evans, M. M. R. & Nogami, J. Indium and gallium on Si(001): A closer look at the parallel dimer structure . *Phys. Rev. B* **59**, 7644–7648 (1999).

16. Nogami, J., Baski, A. A. & Quate, C. F. Aluminum on the Si(100) surface: Growth of the first monolayer. *Phys. Rev. B* **44**, 1415–1418 (1991).

17. Glueckstein, J. C., Evans, M. M. R. & Nogami, J. Growth of Sn on Si(001) at room temperature. *Surf. Sci.* **415**, 80–94 (1998).

18. Itoh, H., Tanabe, H., Winau, D., Schmid, A. K. & Ichinokawa, T. Growth mode and surface structures of the Pb/Si(001) system observed by scanning tunneling microscopy. *J. Vac. Sci. Tech. B* **12**, 2086–2089 (1994).

19. Tomatsu, K., Nakatsuji, K., Iimori, T. & Komori, F. STM observation of initial growth of Sn atoms on Ge(001) surface. *Surf. Sci.* **601**, 1736–1746 (2007).

20. Hutchison, P., Evans, M. M. R. & Nogami, J. Mg growth on the Si(001) surface: An STM study. *Surf. Sci.* **411**, 99–110 (1998).

21. Bakhtizin, R. Z., Kishimoto, J., Hashizume, T. & Sakurai, T. STM study of Sr adsorption on Si(100) surface. *Appl. Surf. Sci.* **94**, 478–484 (1996).

22. Bird, C. F. & Bowler, D. R. A spin polarized first-principles study of short dangling bond wires on Si(001). *Surf. Sci.* **531**, L351–L355 (2003).

23. Chen, T. C. *et al.* Atomic-scale desorption through electronic and vibrational excitation mechanisms. *Science* **268**, 1590–1592 (1995).

24. Cyr, C. M., Venkataraman, B. & Flynn, G. W. Functional group identification in scanning tunneling microscopy of molecular adsorbates. *J. Phys. Chem.* **100**, 13747–13759 (1996).

25. Canas-Ventura, M. E. *et al.* Coexistence of one- and two-dimensional supramolecular assemblies of terephthalic acid on Pd(111) due to self-limiting deprotonation. *J. Chem Phys.* **125**, 184710 (2006).

26. Lopinski, G. P., Wayner, D. D. M. & Wolkow, R. A. Self-directed growth of molecular nanostructures on silicon. *Nature* **406**, 48–51 (2000).

27. DiLabio, G. A., Piva, P. G., Kruse, P. & Wolkow, R. A. Dispersion interactions enable the self-directed growth of linear alkane nanostructures covalently bound to silicon. *J. Am. Chem. Soc.* **126**, 16048–16050 (2004).

28. Kruse, P., Johnson, E. R., DiLabio, G. A. & Wolkow, R. A. Patterning of vinylferrocene on H–Si(100) via self-directed growth of molecular lines and STM-induced decomposition. *Nano Lett.* **2**, 807–810 (2002).

29. Hossain, M. Z., Kato, H. S. & Kawai, M. Controlled fabrication of 1D molecular lines across the dimer rows on the Si(100)-(2 × 1)-H surface through the radical chain reaction. *J. Am. Soc. Chem.* **127**, 15030–15031 (2005).

30. Hossain, M. Z., Kato, H. S. & Kawai, M. Fabrication of interconnected 1D molecular lines along and across the dimer rows on the Si(100)-(2 × 1)-H surface through the radical chain reaction. *J. Phys. Chem. B* **109**, 23129–23133 (2005).

31. Shimomura, M. *et al.* Formation of one-dimensional molecular chains on a solid surface: Pyrazine/Si(001). *Phys. Rev. B* **72**, 033303 (2005).

32. Wang, Y., Chen, X. & Hamers, R. J. Atomic-resolution study of overlayer formation and interfacial mixing in the interaction of phosphorus with Si(001). *Phys. Rev. B* **50**, 4534–4547 (1994).

33. Kipp, L. *et al.* Adsorption and decomposition on Si(100) 2 × 1 studied by STM . *Phys. Rev. B* **52**, 5843–5850 (1995).

34. Knall, J. & Pethica, J. B. Growth of Ge on Si(100) and Si(113) studied by STM. *Surf. Sci.* **265**, 156–167 (1992).

35. Park, Ch., Bakhizin, R. Z., Hashizume, T. & Sakurai, T. Strain relief and ordering of (2 × n)-Bi structure on Si(100). *J. Vac. Sci. Technol. B* **12**, 2049–2051 (1994).

36. Wang, Y. & Hwang, G. S. Two-dimension arrangement of CH$_3$NH$_2$ adsorption on Si(001)-2×1. *Chem. Phys. Lett.* **385**, 144–148 (2004).

37. Wang, Y. & Hwang, G. S. Origin of nonlocal interactions in adsorption of polar molecules on Si(001)-2×1. *J. Chem. Phys.* **122**, 164706 (2005).

38. Gao, Q., Cheng, C. C., Chen, P. J., Choyke, W. J. & Yates, J. T. Jr. Chlorine bonding sites and bonding configurations on Si(100)-2 × 1. *J. Chem. Phys.* **98**, 8308–8323 (1993).

39. Szabo, A., Farrall, P. D. & Engel, T. Reactions of chlorine with Si(100) and Si(111): Adsorption and desorption kinetics. *Surf. Sci.* **312**, 284–300 (1994).

40. Gupta, P., Coon, P. A., Koehler, B. G. & George, S. M. Desorption product yields following Cl$_2$ adsorption on Si(111)-7 × 7: Coverage and temperature dependence. *Surf. Sci.* **249**, 92–104 (1991).

41. Dobrin, S. *et al.* Self-assembled molecular corrals on a semiconductor surface. *Surf. Sci.* **600**, 43–47 (2006).

42. Dubois, M., Delerue, C. & Rubio, A. Adsorption and electronic excitation of biphenyl on Si(100): a theoretical STM analysis. *Phys. Rev. B* **75**, 041302 (2004).

43. Grandidier, B. *et al.* Effect of alkyl substituents on the adsorption of thienylenevinylene oligomers on the Si(100) surface. *Surf. Sci.* **473**, 1–7 (2001).

44. Lei, R. Z., Gellman, A. J. & Koel, B. E. Desorption energies of linear and cyclic alkanes on surfaces: Anomalous scaling with length. *Surf. Sci.* **554**, 125–140 (2004).

45. Dobrin, S. *et al.* Molecular dynamics of haloalkane corral-formation and surface halogenation at Si(111)-7 × 7. *J. Chem. Phys.* **125**, 133407 (2006).

46. Grandidier, B. *et al.* Effect of alkyl substituents on the adsorption of thienylenevinylene oligomers on the Si(100) surface. *Surf. Sci.* **473**, 1–7 (2001).

47. Dubois, M., Delerue, C. & Allan G. Scanning tunneling microscopy and spectroscopy of conjugated oligomers weakly bonded to Si(100) surfaces: A theoretical study. *Phys. Rev. B* **71**, 165435 (2005).

48. Kondo, Y., Amakusa, T., Iwatsuki, M. & Tokomoto, H. Phase transition of the Si(001) surface below 100 K. *Surf. Sci.* **453**, L318–L322 (2000).

49. Lyubinetsky, I., Dohnalek, Z., Choyke, W. J. & Yates, J. T. Jr. Cl$_2$ dissociation on Si(100)-(2 × 1): A statistical study by scanning tunneling microscopy. *Phys. Rev. B* **58**, 7950–7957 (1998).

50. Okada, H., Fujimoto, Y., Endo, K., Hirose, K. & Mori, Y. Detailed analysis of scanning tunneling microscopy images of the Si(001) reconstructed surface with buckled dimers. *Phys. Rev. B* **63**, 195324 (2001).

51. Oura, K., Lifshits, V. G., Saranin, A. A., Zotov, A. V. & Katayama, M. *Surface Science: An Introduction* 181–183 (Springer-Verlag, Berlin, 2003).

52. Bartmess, J. E. & Georgiadis, R. M. Empirical methods for determination of ion gauge sensitivities for different gases. *Vacuum* **33**, 149–153 (1983).

53. Kresse, G. & Hafner, J. *Ab initio* molecular dynamics for liquid metals. *Phys. Rev. B* **47**, 558–561 (1993).

54. Kresse, G. & Furthmüller, J. Efficient iterative schemes for *ab initio* total-energy calculations using a plane-wave basis set. *Phys. Rev. B* **54**, 11169–11186 (1996).

55. Perdew, J. P. *et al.* Atoms, molecules, solids, and surfaces: Applications of the generalized gradient approximation for exchange and correlation. *Phys. Rev. B* **46**, 6671–6687 (1992).

56. Hofer, W. A. & Redinger, J. STM of binary alloys: First principles calculation of the current for PtX(100) surfaces. *Surf. Sci.* **447**, 51–61 (2000).

57. Palotas, K. & Hofer, W. A. Multiple scattering in a vacuum barrier obtained from real-space wavefunctions. *J. Phys. Condens. Matter* **17**, 2705–2713 (2005).

Author contributions

The experiments were performed jointly by K.R.H., T.L., I.R.M. and J.C.P. at the University of Toronto, and the computations by L.Z., S.A. and W.A.H. at the University of Liverpool.